



UNIVERSITY OF LEEDS

This is a repository copy of *CoronARE: A Coronary Artery Reconstruction Challenge*.

White Rose Research Online URL for this paper:

<http://eprints.whiterose.ac.uk/145450/>

Version: Accepted Version

Proceedings Paper:

Çimen, S, Unberath, M, Frangi, A orcid.org/0000-0002-2675-528X et al. (1 more author) (2017) *CoronARE: A Coronary Artery Reconstruction Challenge*. In: *Lecture Notes in Computer Science*, vol 10555. Fifth International Workshop, CMMI 2017, Second International Workshop, RAMBO 2017, and First International Workshop, SWITCH 2017, Held in Conjunction with MICCAI 2017, 14 Sep 2017, Québec City, QC, Canada. Springer Verlag , pp. 96-104. ISBN 978-3-319-67563-3

https://doi.org/10.1007/978-3-319-67564-0_10

© Springer International Publishing AG 2017. This is an author produced version of a paper published in *Lecture Notes in Computer Science*. Uploaded in accordance with the publisher's self-archiving policy.

Reuse

Items deposited in White Rose Research Online are protected by copyright, with all rights reserved unless indicated otherwise. They may be downloaded and/or printed for private study, or other acts as permitted by national copyright laws. The publisher or other rights holders may allow further reproduction and re-use of the full text version. This is indicated by the licence information on the White Rose Research Online record for the item.

Takedown

If you consider content in White Rose Research Online to be in breach of UK law, please notify us by emailing eprints@whiterose.ac.uk including the URL of the record and the reason for the withdrawal request.



eprints@whiterose.ac.uk
<https://eprints.whiterose.ac.uk/>

CoronARe: A Coronary Artery Reconstruction Challenge

Serkan Çimen^{1,*}, Mathias Unberath^{2,*}, Alejandro Frangi¹, and Andreas Maier²

¹ Center for Computational Imaging and Simulation Technologies in Biomedicine
The University of Sheffield, Sheffield, United Kingdom

² Pattern Recognition Lab
Friedrich-Alexander-Universität Erlangen-Nürnberg, Erlangen, Germany

Abstract. *CoronARe* ranks state-of-the-art methods in symbolic and tomographic coronary artery reconstruction from interventional C-arm rotational angiography. Specifically, we benchmark the performance of the methods using accurately pre-processed data, and study the effects of imperfect pre-processing conditions (segmentation and background subtraction errors). In this first iteration of the challenge, evaluation is performed in a controlled environment using digital phantom images, where accurate 3D ground truth is known.

Keywords: Angiography, 3D Reconstruction, C-arm Cone-beam CT, Motion Compensation

1 Introduction

Coronary artery disease (CAD) is a serious illness, which is responsible for approximately 20 % of the deaths in Europe [1] and in the US [2]. Currently, clinical decision regarding the presence and the extent of CAD is taken by the help of several diagnostic and interventional medical imaging modalities. Among those, invasive (catheter-based) X-ray coronary angiography is still the most common choice for the assessment of CAD. Owing to its high spatial/temporal resolution and its availability, it is still considered as the gold standard in clinical decision making and therapy guidance [3].

The X-ray angiography systems evolved continuously since their first introduction almost five decades ago. However, X-ray coronary angiography is known to be fundamentally limited due to the projective 2D representation of the coronary artery trees with complex anatomy and motion. Misinterpretation of lesion lengths, eccentricity, angles of bifurcations and vessel tortuosity due to the 2D nature of the X-ray angiography could lead to over/under estimation of lesion severity and incorrect selection of stent size [4, 5]. Methods computing reconstructions of coronary arteries from X-ray angiography aim to overcome this shortcoming by providing 3D information of the coronary arteries. Due to the

* Both authors contributed equally to this paper.

complexity of this task, the topic of reconstruction from X-ray coronary angiography remains as a challenging and active research area.

Public benchmarks contribute to drive forward this area as they allow for objective comparison of coronary artery reconstruction algorithms from rotational angiography. A previous effort, *CAVAREV* [6] laid the foundation for public benchmarks in this field but is limited to tomographic reconstruction algorithms. Within the *CoronARe* challenge, we seek to continue the *CAVAREV* incentive by providing a public benchmark for both tomographic and symbolic reconstruction algorithms. In this first iteration of the challenge, we study current state-of-the-art reconstruction algorithms in a highly controlled setup on numerical phantom data, where accurate 3D and 2D data is available.

2 Material and Methods

2.1 Scope and Specific Goals

The literature is divided into symbolic (i. e. model-based) and tomographic methods [7]. Symbolic reconstruction algorithms try to recover a binary representation of the topology of the arterial tree while tomographic reconstruction methods directly reconstruct the 3D volume of attenuation coefficients. Irrespective of their categorization as symbolic or tomographic, most currently known coronary artery reconstruction algorithms from rotational angiography rely on projection domain vessel segmentation or centerline extraction algorithms to either perform background suppression or obtain sparse data. Much work has considered automatic vessel segmentation [7–9] both in an analytic, model-based but also in a machine learning context. While results are promising when a static imaging geometry can be assumed (e. g. as in traditional angiography), satisfactory segmentation quality cannot yet be reliably achieved in rotational angiography because of substantial changes in vessel visibility in successive views due to overlap with high contrast structures, such as the spine.

Consequently, automatic segmentation algorithms inevitably lead to projection domain mis-segmentations and inconsistencies (which we will refer to as corruption) that have to be addressed during reconstruction. Within the challenge described here, we investigate how different methods cope with imperfect pre-processing of the projection images, i. e. errors in centerline segmentation and single-frame background subtraction based on vessel segmentation and inpainting. The setup of the challenge is described in greater detail in the remainder of this manuscript.

2.2 Data

Numerical Phantom To create the controlled setup for benchmarking the reconstruction algorithms, we decided to use the 4D XCAT Phantom [10]. This phantom defines detailed and anatomically correct cardiac vasculature using non-uniform rational B-splines (NURBS). It also allows for the simulation of

cardiac motion.

The left coronary artery (LCA) geometry of the XCAT phantom is used to generate the projection data for both symbolic and tomographic reconstruction parts of this challenge. A sequence of 133 NURBS descriptions of the LCA is simulated for the whole acquisition duration, where we set the heart rate to 80 beats per minute.

For the symbolic reconstruction, 3D ground truth is obtained by sampling the spline defining the centerlines at regular arc length intervals of 0.3 mm. For each projection in the sequence, the 3D spline is projected onto the corresponding image plane. Similar to 3D, points defining the uncorrupted centerline segmentations are sampled from these splines at regular arc length intervals of 2.0 mm. In addition, the sequence of NURBS files are voxelized with an isotropic image spacing of 0.3 mm, and the values of the voxels corresponding to artery locations set to one, whereas remaining voxels are set to zero. A subvolume of size $512 \times 512 \times 360$ centered at the barycenter of the 3D ground truth points of the end-diastolic phase defines the ground truth for each time step in the sequence. The CT Projector [10] is used to simulate the projection images, which is capable of computing the sum of attenuation values analytically from NURBS definitions given the imaging geometry.

Imaging Geometry The 4D numerical phantom is forward projected using the geometric calibration of a real scanner taken from *CAVAREV* [6] describing a standard rotational angiography protocol. In particular, 133 images are acquired during a single 5.3s sweep on a circular source trajectory covering 200° . The projection images have a size of 960×960 pixels in horizontal and vertical direction, respectively, with an isotropic size of 0.32 mm. The source-to-isocenter and source-to-detector distances nominally are 800 mm and 1200 mm, respectively.

Artificial Corruption: Imperfect Preprocessing Within this challenge, corruption of the acquisition will be random but with increasing severity. Particularly, for both the symbolic and tomographic data sets we use the uncorrupted acquisitions as the baseline and add excessive structure such that the corruption amounts to 10 %, 20 %, and 30 % of the true information [11].

Symbolic Reconstruction It is well known that the reconstruction problem in rotational angiography is ill-posed due to high frequency cardiac motion. Symbolic reconstruction algorithms exploit sparsity of the vessel centerlines to overcome this challenge suggesting that reconstruction results heavily depend on the quality of the centerlines.

To realistically simulate vessel extraction errors, points were sampled from random curves, and added to the true segmentation points following [11]. Specifically, random trajectories of particles were generated using Brownian motion, and smoothed by fitting cubic Hermite splines. The points corresponding to the

vessel extraction errors were sampled from these splines at 2.0 mm, which is the same rate used for generating the true centerline segmentation.

Tomographic Reconstruction Background subtraction or -suppression proved highly beneficial for reconstruction quality when considering both analytic and algebraic reconstruction algorithms [7], as it promotes sparsity and corrects for truncation [12]. This preprocessing step usually relies on binary masks of the target vessels to identify the contrasted lumen and, subsequently, virtually remove the background.

We simulate errors in the suppression process by generating a corruption image for each projection in the sequence, and adding it to the corresponding uncorrupted image. The same random points generated for symbolic reconstruction were employed in this process. To this end, these random points were first converted into a binary image. This image was smoothed by a Gaussian filter, and the intensity values were rescaled so that the maximum intensity value equals to the mean of the non-zero pixels in the corresponding uncorrupted image.

Examples of background subtracted projection images and corresponding centerline segmentations at varying levels of corruption were shown in Figure 1.

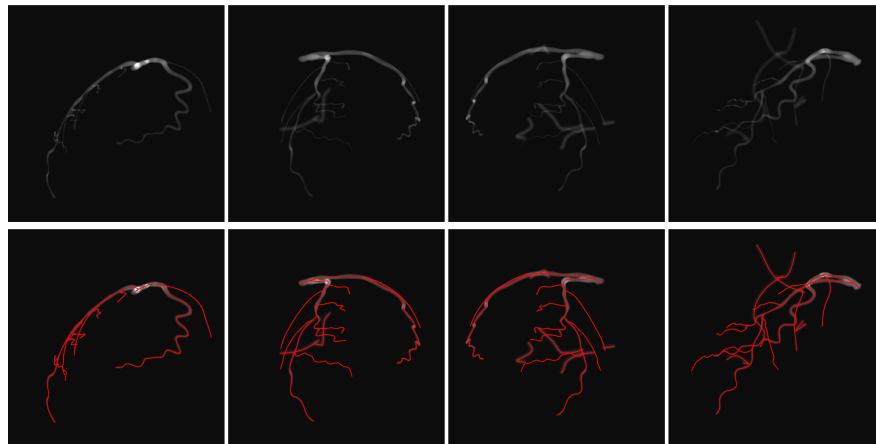


Fig. 1. Examples of the projection images at different corruption levels and from different views. (a)-(d) Projection images at 0%, 10%, 20%, and 30% corruption levels, respectively. (e)-(h) The centerline segmentations provided for the symbolic reconstruction were overlaid on the corresponding projection images.

Public Challenge Input Data Finally, after generation of the projection domain data (i. e. images and centerline points) and artificial corruption thereof we provide the following data set as designated input to candidate reconstruction algorithms:

- **Background-subtracted projection images:** We provide background subtracted line-integral data of the contrasted coronary arteries at varying levels of corruption. The data is stored as meta-image [13] with detached headers. For analytic, FDK-type [14] reconstruction algorithms, we provide pre-processed versions of the line-integral images in the same format.
- **Densely sampled projection domain centerline points:** Projection domain centerlines at the four corruption levels are provided in separate text files, where the horizontal and vertical detector coordinates of a particular centerline point are whitespace separated and occupy one row each.
- **Cardiac phase data:** The relative cardiac phases are stored in a simple text file. The phases are periodic and in the interval $[0, 1[$, where $0 \equiv 1$ represents a phase at the end of ventricular diastole.
- **Projection matrices:** We provide projection matrices $P_i \in \mathbb{R}^{3 \times 4}$ that encode the imaging geometry [15] and map from 3D world to 2D image coordinates. The matrix entries are stored as floats in a single binary file containing the 133 matrices in row-major order.

For a more detailed description of the provided data kindly refer to the particular section of this manuscript or the *CoronARe* challenge homepage³, where we also link to exemplary code that provides guidance on how to handle the data.

2.3 Evaluation Protocol and Ranking

Tomographic Reconstruction Scoring of tomographic reconstructions relies on *3D volumetric overlap*.

The input volume arising from tomographic reconstruction is repeatedly binarized using a sweeping threshold within the interval $[0, 255]$ [6]. The binary volume is then compared to the segmentation mask of the ground-truth morphology using the Dice similarity coefficient [16], a common two-sided measure for the overlap of two binary images ranging from zero (no overlap) to one (perfect match). As the final score, it selects the best value over all thresholds.

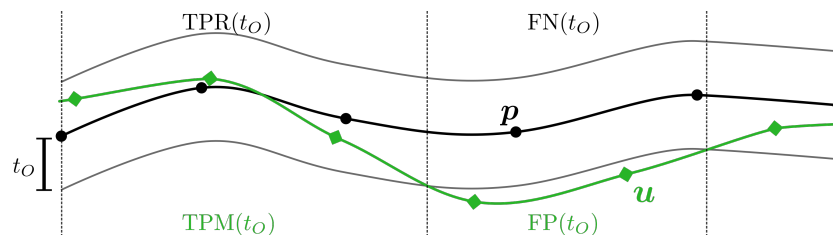


Fig. 2. Schematic illustration of the 3D reconstruction overlap curve computation. 3D points of the test and ground truth centerlines are labeled as true and false positives or negatives depending on the sweeping test distance t_0 .

³ Visit <https://www5.cs.fau.de/research/software/coronare/>.

Symbolic Reconstruction Scoring of symbolic centerline reconstructions relies on *3D reconstruction overlap curves*.

For a particular combination of ground truth and test centerline points, \mathcal{P}_G and \mathcal{P}_S , respectively, the procedure is as follows.

To assess the overlap of a input reconstruction with the 3D ground truth we use a sweeping distance threshold $t_O \in [t_{\min}, t_{\max}]$ rather than the vessel diameter. Given a distance t_O , every point of the ground truth $\mathbf{p} \in \mathcal{P}_G$ is marked as belonging to the set $\text{TPR}(t_O)$ of true positives of the reference if there is at least one point $\mathbf{u} \in \mathcal{P}_S$ satisfying $d(\mathbf{p}, \mathbf{u}) < t_O$ and to the set $\text{FN}(t_O)$ of false negatives otherwise. Points of the reconstruction \mathbf{u} are labeled as belonging to the set $\text{TPM}(t_O)$ of true positives of the tested method if there is at least one ground truth point \mathbf{p} satisfying $d(\mathbf{u}, \mathbf{p}) < t_O$ and to the set $\text{FP}(t_O)$ of false positives otherwise. An schematic of the labeling process is provided in Figure 2. The overlap for a certain distance can then be computed as

$$O(t_O) = \frac{|\text{TPM}(t_O)| + |\text{TPR}(t_O)|}{|\text{TPM}(t_O)| + |\text{TPR}(t_O)| + |\text{FN}(t_O)| + |\text{FP}(t_O)|} . \quad (1)$$

Similar to the Dice score, the overlap measure ranges from zero (no overlap) to one (perfect match). With increasing distance thresholds the measure increases monotonically. A simple score that reflects the overall quality of a reconstruction is the area under the overlap curve

$$\tilde{O} = \frac{1}{t_{\max} - t_{\min}} \int_{t_{\min}}^{t_{\max}} O(t) dt \quad (2)$$

that, again, ranges from zero to one indicating no to perfect overlap, respectively. A reasonable choice may be $(t_{\min}, t_{\max}) = (0 \text{ mm}, 1 \text{ mm})$.

2.4 Ranking

Our challenge design accommodates symbolic (i. e. centerline only) and tomographic coronary artery reconstruction. As the output of algorithms from both categories is substantially different, we perform a separate ranking of symbolic and tomographic algorithms.

Particularly, we select the best tomographic and symbolic methods with respect to overall reconstruction performance (averaged over all input data corruption levels) and with respect to clean data reconstruction performance.

Currently, there is no separate category for methods that incorporate external information, e. g. by using learning-based algorithms. The organizers emphasize that, in such cases, the XCAT anatomy must be excluded from the training and validation set.

2.5 Submission Guidelines and Formats

Partial participation (e. g. tomographic reconstruction, clean data only) is possible.

Although we provide full rotational angiography data, we highly encourage the participation of algorithms that do not operate on the complete data set, such as reconstruction from bi-plane data that is artificially created from the provided sequence.

The winners of the first phase of *CoronARe* were announced during an oral session at the *Reconstruction of Moving Body Organs (RAMBO)*⁴ workshop that was held in conjunction with the *20th International Conference on Medical Image Computing and Computer Assisted Intervention (MICCAI) 2017*⁵. Evaluation within *CoronARe* is fully automated as it hosted using Kitware’s Covalic [17]. Consequently, data download, result submission, and ranking remains possible even after the official completion of the first phase.

Submission formats for tomographic and symbolic reconstructions are held as simple as possible. For tomographic data we rely on the previously established *CAVAREV* format. For symbolic reconstruction we use a simple text file format where the coordinates of every 3D centerline point are whitespace separated and occupy one row each.

For a more detailed description of the submission file formats including example code for the tomographic format kindly refer to the *CoronARe* challenge homepage⁶.

3 Discussion and Outlook

We are aware and convinced of the fact that ranking of coronary artery reconstruction methods ultimately is most meaningful on clinical patient data, as such data imposes difficulties that are not sufficiently captured by in silico phantoms, such as anatomical variations (i.e. generalization). However, there is no joint benchmark for tomographic and symbolic reconstruction, even in a simple, controlled experimental setup. Moreover, the effects of corrupted projection domain data onto the reconstruction quality are not yet sufficiently understood. This challenge is meant to overcome these shortcomings, and to have a better understanding of the problem for future challenges that should be carried out on clinical data.

In conclusion, this challenge constitutes yet another effort in providing data and means of objective comparison. We hope to publish our findings of this first submission phase in a comprehensive journal article, ranking methods of the current state-of-the-art. In tomographic reconstruction, we would be particularly interested in understanding how motion compensation strategies compare to algebraic methods that exploit prior knowledge on image appearance. When considering symbolic reconstruction methods, we believe that a comparison between bi-plane and multi-view reconstruction algorithms is of substantial interest.

Both data and submission will remain available even after closure of the initial submission phase. We hope this data to be helpful in future publications of

⁴ Visit <https://sites.google.com/view/miccai-rambo2017/home>.

⁵ Visit <http://www.miccai2017.org/>.

⁶ Visit <https://www5.cs.fau.de/research/software/coronare/>.

peers, ideally, as a highly competitive benchmark of tomographic and symbolic coronary artery reconstruction algorithms.

Acknowledgement

The authors would like to thank Zach Mullen, Kitware, for his support in hosting this challenge.

References

1. Nichols, M., Townsend, N., Scarborough, P., Rayner, M.: Cardiovascular disease in Europe: epidemiological update. *European Heart Journal* **34**(39) (2013) 3028–3034
2. Go, A.S., Mozaffarian, D., Roger, V.L., Benjamin, E.J., Berry, J.D., Blaha, M.J., Dai, S., Ford, E.S., Fox, C.S., Franco, S., et al.: Heart disease and stroke statistics – 2014 update. *Circulation* **129**(3) (2014)
3. Mark, D.B., Berman, D.S., Budoff, M.J., Carr, J.J., Gerber, T.C., Hecht, H.S., Hlatky, M.A., Hodgson, J.M., Lauer, M.S., Miller, J.M., et al.: ACCF/ACR/AHA/NASCI/SAIP/SCAI/SCCT 2010 expert consensus document on coronary computed tomographic angiography. *Catheterization and Cardiovascular Interventions* **76**(2) (2010) E1–E42
4. Gollapudi, R.R., Valencia, R., Lee, S.S., Wong, G.B., Teirstein, P.S., Price, M.J.: Utility of three-dimensional reconstruction of coronary angiography to guide percutaneous coronary intervention. *Catheterization and Cardiovascular Interventions* **69**(4) (2007) 479–482
5. Eng, M.H., Hudson, P.A., Klein, A.J., Chen, S.J., Kim, M.S., Groves, B.M., Messenger, J.C., Wink, O., Carroll, J.D., Garcia, J.A.: Impact of Three Dimensional In-Room Imaging (3DCA) in the Facilitation of Percutaneous Coronary Interventions. *Journal of Cardiology and Vascular Medicine* **1**(1) (2013) 1
6. Rohkohl, C., Lauritsch, G., Keil, A., Hornegger, J.: CAVAREV—an open platform for evaluating 3D and 4D cardiac vasculature reconstruction. *Physics in Medicine and Biology* **55**(10) (2010) 2905
7. Çimen, S., Gooya, A., Grass, M., Frangi, A.F.: Reconstruction of coronary arteries from X-ray angiography: A review. *Medical Image Analysis* **32** (2016) 46–68
8. Dehkordi, M.T., Sadri, S., Doosthoseini, A.: A review of coronary vessel segmentation algorithms. *Journal of Medical Signals and Aensors* **1**(1) (2011) 49
9. Unberath, M., Taubmann, O., Hell, M., Achenbach, S., Maier, A.: Symmetry, Outliers, and Geodesics in Coronary Artery Centerline Reconstruction from Rotational Angiography. *Medical Physics* (2017) (in press).
10. Segars, W.P., Sturgeon, G., Mendonca, S., Grimes, J., Tsui, B.M.W.: 4D XCAT phantom for multimodality imaging research. *Medical Physics* **37**(9) (2010) 4902–15
11. Çimen, S., Gooya, A., Ravikumar, N., Taylor, Z.A., Frangi, A.F.: Reconstruction of Coronary Artery Centrelines from X-Ray Angiography Using a Mixture of Student’s t-Distributions. In: *Proc. Medical Image Computing and Computer Assisted Intervention (MICCAI) 2016*, Springer (2016) 291–299
12. Unberath, M., Aichert, A., Achenbach, S., Maier, A.: Consistency-based Respiratory Motion Estimation in Rotational Angiography. *Medical Physics* (2017) (in press).

13. Public, K.: MetaIO Documentation. <https://itk.org/Wiki/ITK/MetaIO/Documentation> (2014) Accessed: 2017-06-09.
14. Feldkamp, L.A., Davis, L.C., Kress, J.W.: Practical cone-beam algorithm. *Journal of the Optical Society of America A* **1**(6) (1984) 612–619
15. Hartley, R., Zisserman, A.: Multiple view geometry in computer vision. 2 edn. Cambridge University Press (2004)
16. Sørensen, T.: A method of establishing groups of equal amplitude in plant sociology based on similarity of species and its application to analyses of the vegetation on danish commons. *Biologiske Skrifter* **5** (1948) 1–34
17. Public, K.: Colvalic. <https://challenge.kitware.com/> Accessed: 2017-07-09.